

# *HST* ABSOLUTE PROPER MOTIONS OF NGC 6681 (M70) AND THE SAGITTARIUS DWARF SPHEROIDAL GALAXY\*

D. Massari<sup>1</sup>, A. Bellini<sup>2</sup>, F. R. Ferraro<sup>1</sup>, R. P. van der Marel<sup>2</sup>, J. Anderson<sup>2</sup>, E. Dalessandro<sup>1</sup>, and B. Lanzoni<sup>1</sup>

May 24, 2022

## ABSTRACT

We have measured absolute proper motions for the three populations intercepted in the direction of the Galactic globular cluster NGC 6681: the cluster itself, the Sagittarius dwarf spheroidal galaxy and the field. For this we used *Hubble Space Telescope* ACS/WFC and WFC3/UVIS optical imaging data separated by a temporal baseline of 5.464 years. Five background galaxies were used to determine the zero point of the absolute-motion reference frame. The resulting absolute proper motion of NGC 6681 is  $(\mu_\alpha \cos \delta, \mu_\delta) = (1.58 \pm 0.18, -4.57 \pm 0.16)$  mas yr<sup>-1</sup>. This is the first estimate ever made for this cluster. For the Sgr dSph we obtain  $(\mu_\alpha \cos \delta, \mu_\delta) = (-2.54 \pm 0.18, -1.19 \pm 0.16)$  mas yr<sup>-1</sup>, consistent with previous measurements and with the values predicted by theoretical models. The absolute proper motion of the Galaxy population in our field of view is  $(\mu_\alpha \cos \delta, \mu_\delta) = (-1.21 \pm 0.27, -4.39 \pm 0.26)$  mas yr<sup>-1</sup>. In this study we also use background Sagittarius Dwarf Spheroidal stars to determine the rotation of the globular cluster in the plane of the sky and find that NGC 6681 is not rotating significantly:  $v_{\text{rot}} = 0.82 \pm 1.02$  km s<sup>-1</sup> at a distance of 1' from the cluster center.

*Subject headings:* proper motions: general; globular clusters: individual (NGC 6681); dwarf galaxies: individual (Sagittarius Dwarf Galaxy)

## 1. INTRODUCTION

Galactic Globular Clusters (GCs) provide a powerful tool to investigate the structure and the formation history of the Milky Way. Indeed, they are fundamental probes of the Galactic gravitational potential shape, from the outer region of the Galaxy (see Casetti-Dinescu et al. 2007) to the inner Bulge (Casetti-Dinescu et al. 2010). The currently and most widely accepted picture for the formation of the Galactic GC system (Zinn 1993, Forbes & Bridges 2010) points

toward an accreted origin for the outer ( $r > 10$  kpc) young halo (YH) GCs, while a large number of the inner, old halo (OH) clusters probably formed via dissipationless collapse, coevally with the collapse of the protogalaxy. The finding of several OH, metal-poor GCs with a thick disc-like kinematics (Dinescu et al. 1999), sets a tight constraint on the epoch of the formation of the Galactic disc. Moreover, the demonstration that several YH GCs are kinematically associated with satellites of the Milky Way, such as the Sagittarius dwarf spheroidal galaxy (hereafter Sgr dSph, see for instance Bellazzini et al. 2003), gives important clues as to how the Galaxy was built up through merger episodes. The Sgr dSph (Ibata et al. 1994, Bellazzini et al. 1999) also provides one of the best opportunities to study the shape, orientation and mass of the Milky Way dark matter halo through investigation of its luminous tidal streams. Recent studies have high-

<sup>1</sup>Dipartimento di Fisica e Astronomia, Università degli Studi di Bologna, v.le Berti Pichat 6/2, I-40127 Bologna, Italy

<sup>2</sup>Space Telescope Science Institute, 3700 San Martin Drive, Baltimore, MD 21218, USA

\*Based on archival observations with the NASA/ESA *Hubble Space Telescope*, obtained at the Space Telescope Science Institute, which is operated by AURA, Inc., under NASA contract NAS 5-26555.

lighted a so-called halo conundrum (Law et al. 2005), showing that the available models were not able to reproduce simultaneously the angular position, distance and radial-velocity trends of leading tidal debris. Law & Majewski (2010) claim to have solved this conundrum by introducing a non-axisymmetric component to the Galactic gravitational potential that can be described as a triaxial halo perpendicular to the Milky Way disc. Even if poorly motivated within the current Cold Dark Matter paradigm, these findings have subsequently been confirmed by Deg & Widrow (2013). However, Debattista et al. (2013) fail to reproduce plausible models of disc galaxies using such a scenario. In order to make substantial progress towards a solution of this debate, new observational data are needed, starting from accurate proper motions (PMs).

The existence of other peculiar systems like  $\omega$  Centauri (Norris & Da Costa 1995) and Terzan 5 (Ferraro et al. 2009) harboring stellar populations with significant iron-abundance differences ( $\Delta[\text{Fe}/\text{H}] > 0.5$  dex) supports a complex formation scenario for the Galactic halo and the Bulge. Therefore, a detailed description of the kinematical properties of the Galactic GC system is a crucial requirement to obtain new and stronger constraints on the formation history of our Galaxy. In this sense, publicly-available catalogs of absolute PMs for several Galactic GCs are of great importance. A notable example is the ground-based Yale/San Juan Southern Proper Motion catalog (Platais et al. 1998, Dinescu et al. 1997 and the following papers of the series). These kinds of studies are extremely difficult in regions of the sky where different stellar populations overlap (such as towards the Bulge) and the associated uncertainties are typically large, ranging between  $0.4 \text{ mas yr}^{-1}$  and  $0.9 \text{ mas yr}^{-1}$  (Casetti-Dinescu et al. 2007, Casetti-Dinescu et al. 2010). In this sense the *Hubble Space Telescope* (*HST*) provides a unique opportunity to measure high-accuracy stellar PMs even in the most crowded and complex regions of the Galaxy, as seen in Clarkson et al. (2008) or Anderson & van der Marel (2010), for example.

As part of a project aimed at using blue straggler stars as tracers of the dynamical evolution of GCs (Ferraro et al. 2009, 2012) we obtained WFC3 observations of the globular cluster

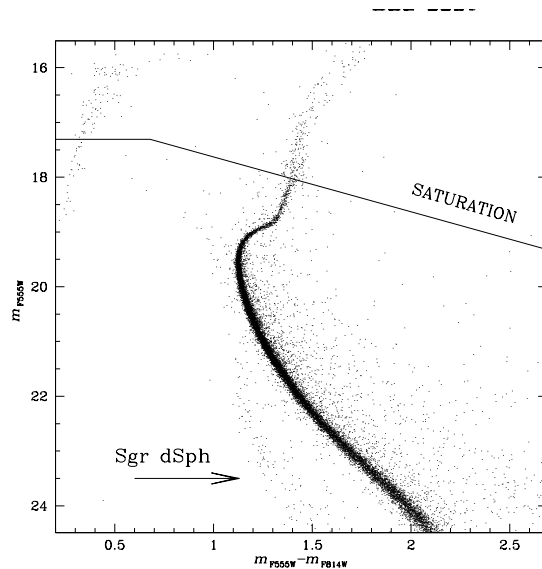


Fig. 1.— The  $(m_{\text{F555W}}, m_{\text{F555W}} - m_{\text{F814W}})$  UVIS/WFC3 CMD of NGC 6681. All of the evolutionary sequences of the cluster are well defined. The broadening of the RGB and the HB is due to exceeding the saturation level, indicated in the plot. The presence of the MS of the Sgr dSph at  $m_{\text{F555W}} > 21$  mag and  $1.1 < m_{\text{F555W}} - m_{\text{F814W}} < 1.8$  mag and the contribution of the field are also evident.

NGC 6681. In this paper we present and discuss accurate PMs of stars in the cluster’s direction. This paper is part of, and uses techniques developed in the context of, the HSTPROMO collaboration,<sup>1</sup> a set of HST projects aimed at improving our dynamical understanding of stars, clusters, and galaxies in the nearby Universe through measurement and interpretation of proper motions. As it happens, NGC 6681 is located in an extremely interesting region of the sky: it overlaps the main body of the Sgr dSph. With the extraordinarily high photometric and astrometric accuracy of *HST* we have been able to separate the two populations and measure their individual absolute PMs. This is the first time that the PM of NGC 6681 has been estimated.

The paper is structured as follows: in Section 2 we describe the *HST* data sets used for our investigation, providing a brief summary of our data-reduction procedure; in Section 3 the relative

<sup>1</sup>For details see HSTPROMO home page at <http://www.stsci.edu/~marel/hstpromo.html>

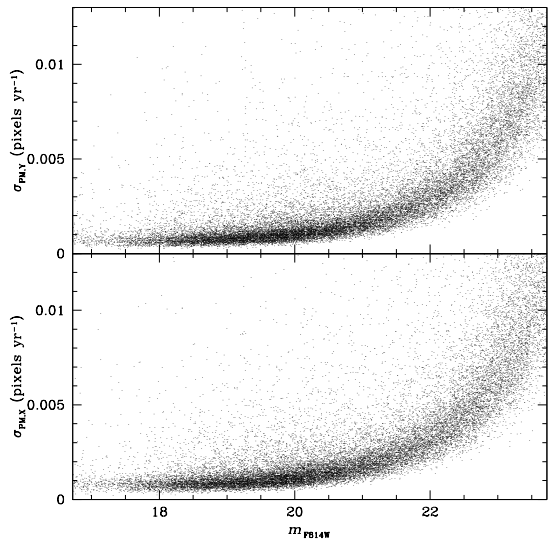


Fig. 2.— Uncertainties, in units of  $\text{pixel yr}^{-1}$ , of the relative PMs along the Y-direction (upper panel) and the X-direction (lower panel), as a function of the  $m_{F814W}$  magnitude. For stars brighter than  $m_{F814W} \sim 20.7$  mag the bulk of the PM uncertainties are smaller than  $0.002 \text{ pixel yr}^{-1}$ .

PMs of our sources are presented; in Section 4 we describe our method for obtaining absolute PMs, by defining the zero-point reference frame and by quantifying possible systematic errors; finally, in Section 5 we present the results of our analysis.

## 2. OBSERVATIONS AND DATA REDUCTION

In order to measure the PMs in the direction of NGC 6681 we used two *HST* data sets. The one used as first epoch was acquired under GO-10775 (PI: Sarajedini). It consists of a set of high-resolution images obtained with the Wide Field Channel (WFC) of the Advanced Camera for Survey (ACS). The WFC/ACS is made up of two  $2048 \times 4096$  pixel detectors with a pixel scale of  $\sim 0.05'' \text{ pixel}^{-1}$  and separated by a gap of about 50 pixels, for a total field of view (FoV) of  $\sim 200'' \times 200''$ . For our investigation we used four deep exposures in both the F606W and the F814W filters (with exposure times of 140 sec and 150 sec, respectively), taken on May 20, 2006. We work here exclusively with the `_FLC` images, which have been corrected with the pixel-based correc-

tion in the pipeline (Anderson & Bedin 2010, and Ubeda & Anderson 2012).

The second-epoch data set is composed of proprietary data obtained through GO-12516 (PI: Ferraro). This program consists of several deep, high-resolution images taken with the UVIS channel of the Wide Field Camera 3 (WFC3) in the F390W, F555W and F814W filters. The WFC3 UVIS camera is made of two  $2048 \times 4096$  pixel chips, separated by a gap of approximately 30 pixels. Its pixel scale is  $\sim 0.04'' \text{ pixel}^{-1}$  and the total FoV is  $162'' \times 162''$ . The sample analyzed in this work consists of  $9 \times 150$  s images in F555W and  $13 \times 348$  s images in F814W. These images have not been corrected for CTE losses, since no pixel-based correction was available at the time of this reduction. These images were taken relatively soon after installation and background in these images is greater than 12 electrons, so any CTE losses should be small, particularly for the bright stars we are focusing on here (see Anderson et al. 2012). Since these observations were taken on November 5, 2011, the two data sets provide a temporal baseline of  $\sim 5.464$  yrs.

The data-reduction procedures are described in detail in Anderson & King (2006). Here we provide only a brief description of the main steps of the analysis. The first step was to reduce each individual exposure. We analyzed the first epoch with the publicly available program `img2xym_WFC.09x10`, which is documented in Anderson & King (2006). This program uses a pre-determined model of spatially varying PSFs plus a single time-dependent perturbation PSF (to account for focus changes or spacecraft breathing). The final output is a catalog with instrumental positions and magnitudes for each exposure. We followed the same approach for the second epoch, by using the program `img2xym_wfc3uv`, which is similar to the ACS program described above. We corrected the star positions in each catalog for geometric distortion, by means of the solution provided by Anderson (2007) for the ACS camera and by Bellini et al. (2011) for the WFC3.

As a consistency check, we built the WFC3/UVIS ( $m_{F555W}$ ,  $m_{F555W} - m_{F814W}$ ) CMD of NGC 6681. The F555W sample was constructed by selecting stars in common among at least 4 out of 9 single-exposure catalogs, while the F814W sample is made up of those stars detected in at

NGC 6681: 5.464-yr proper motions (mas/yr)

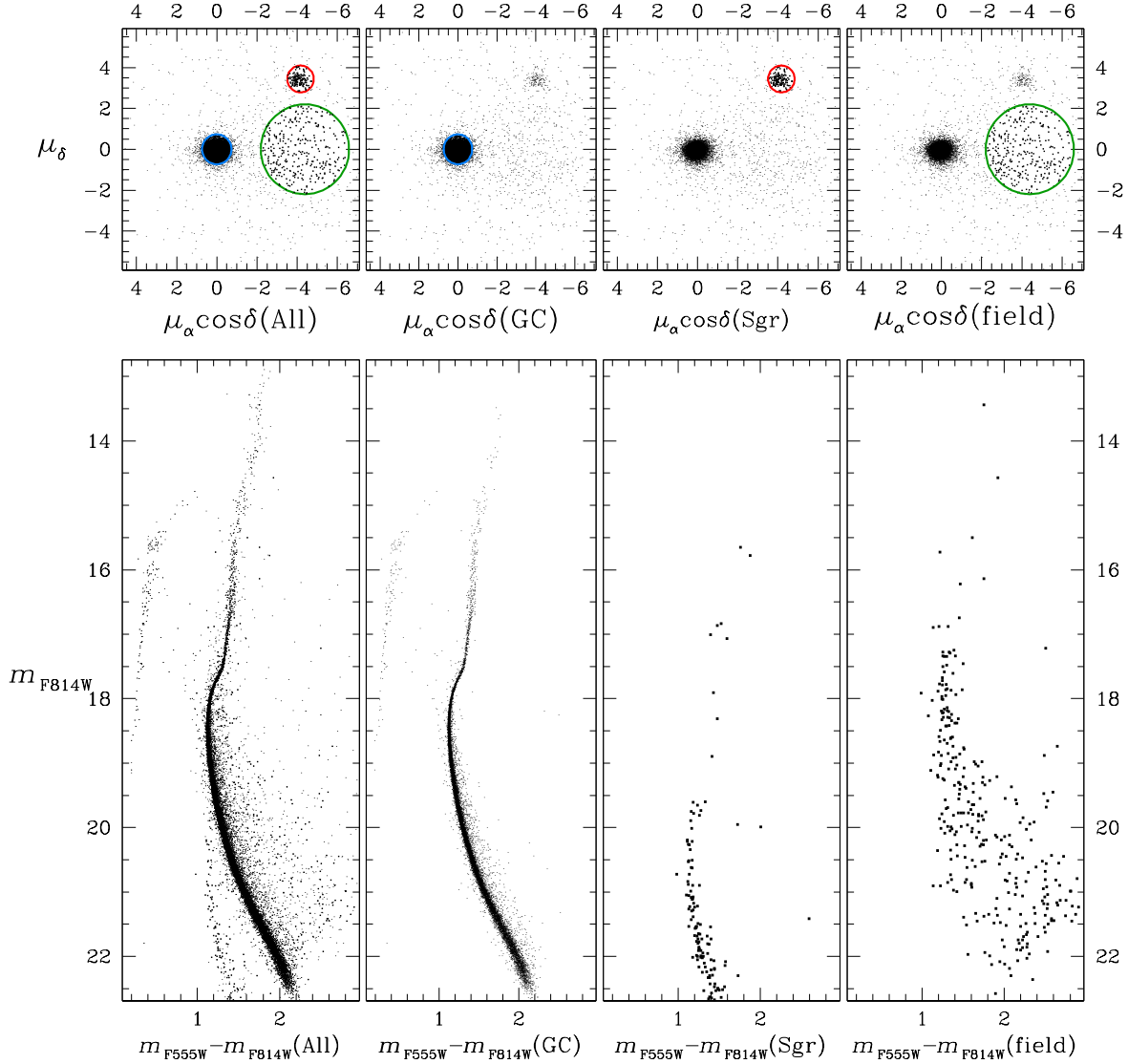


Fig. 3.— The upper panels show the Vector Point Diagrams (VPDs) of the relative PMs. In the lower panels the CMDs corresponding to the selections applied in the VPDs are displayed. *First column:* in the VPD the different populations are indicated with different colors (a sample of cluster members in blue, of Sgr dSph stars in red, of the field in green), but no selection is applied. The corresponding CMD shows the entire PM catalog. *Second column:* in the VPD cluster members are selected within the blue circle and the corresponding CMD displays only well-defined cluster evolutionary sequences. *Third column:* Sgr dSph selection within the red circle and corresponding CMD. *Fourth column:* the selection in the VPD (in green) of the bulk-motion of field stars and their location on the CMD.

least 5 out of 13 single-exposure catalogs. The CMD resulting from these two samples is shown in Figure 1. The instrumental magnitudes have

been calibrated onto the VEGAMag system using aperture corrections and zeropoints reported in

the WFC3 web page<sup>2</sup>. The CMD exhibits well-defined cluster evolutionary sequences. The main sequence (MS) extends to almost 5 magnitudes below the Turn Off (TO) region. Another bluer sequence is visible at  $m_{F555W} > 21$  mag and  $1.1 < m_{F555W} - m_{F814W} < 1.8$  mag and remains well separated from the cluster MS. In the following sections we will demonstrate, by means of PM membership, that it corresponds to the MS of the Sgr dSph (see Siegel et al. 2011). The red giant branch (RGB) and the horizontal branch (HB) of the cluster are almost entirely above the saturation limit and thus are excluded from the PM analysis. A more detailed analysis of the stellar populations in NGC 6681 will be presented in a forthcoming paper.

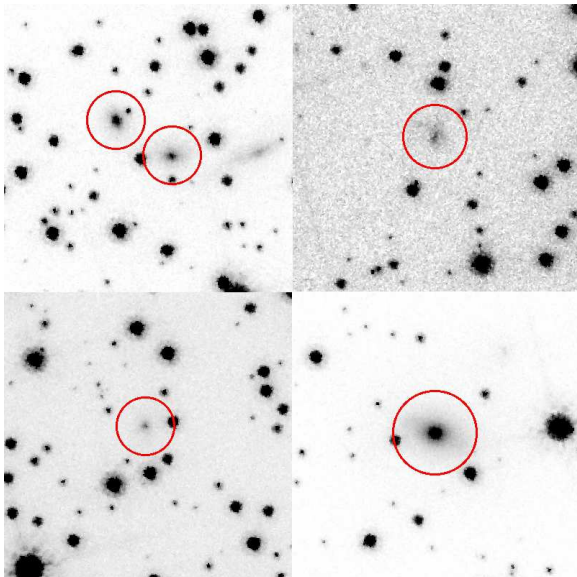


Fig. 4.— The five selected background galaxies as they appear in the F814W images. They differ from the stellar sources since their light is more diffuse across the surrounding pixels. Their point-like nuclei allow us to accurately determine their centroid and thus to obtain a precise measure of their relative proper motions.

### 3. RELATIVE PROPER MOTIONS

The first step in measuring relative PMs was to astrometrically relate each exposure to a distortion-free reference frame, which from now

<sup>2</sup>[http://www.stsci.edu/hst/wfc3/phot\\_zp\\_lbn](http://www.stsci.edu/hst/wfc3/phot_zp_lbn).

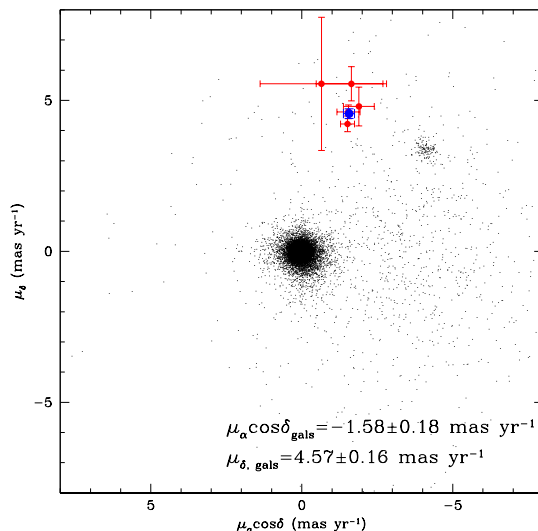


Fig. 5.— Position of the five selected galaxies in the VPD of the relative PMs. They are shown as red dots. The errorbars correspond to the uncertainty of their motions. Their weighted mean position is shown as a blue dot together with its uncertainties and represents the adopted zero point of the absolute-motion reference frame.

on we will refer to as the master frame. We chose the public catalog of NGC 6681 provided by the ACS survey of Galactic GCs (Sarajedini et al. 2007, Anderson et al. 2008) as the master frame. We re-scaled this to the UVIS pixel-scale ( $40 \text{ mas pixel}^{-1}$ ) for convenience. We transformed the measured position of each star in each exposure into the reference frame by means of a six-parameter linear transformation based on the positions of member stars in the reference frame and the individual frames. To maximize the accuracy of these transformations we treated each chip of our exposures separately, in order to avoid spurious effects related to the presence of the gap.

As a second step, we selected a sample of reference stars with respect to which our PMs would be computed. For convenience, we chose to compute all PMs relative to the mean motion of the cluster. Therefore our reference list is based on likely cluster members. These were initially selected on the basis of their location on the CMD. We included in the list only well-measured, unsaturated stars. Then, for each star in each catalog, we computed

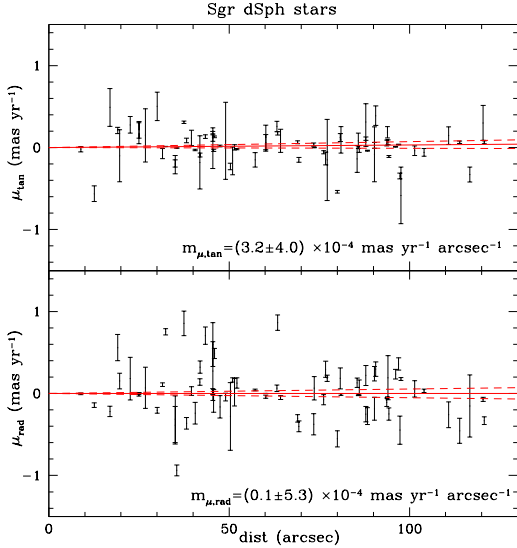


Fig. 6.— *Upper panel*: distribution of the tangential PM component of the Sgr dSph members vs. their angular distance from the NGC 6681 center. The best fit of the functional form  $f = mr$  is shown as a red solid line. The  $1\sigma$  uncertainties are traced as dashed red lines. The labels indicate the value of the best fit slope. *Lower panel*: the same for the radial PM component.

the position on the master frame using a transformation based on only the closest 50 reference stars.

At the end of the process, for each star we have up to 8 first-epoch positions and up to 22 second-epoch positions on the master frame. To estimate the relative motion of each star we adopted a  $3\sigma$ -clipping algorithm and computed the median X and Y positions of each star in the first and in the second epoch. The difference between the two median positions gives the star’s X and Y displacements in  $\Delta T = 5.464$  years. The errors in each direction and within each epoch ( $\sigma_{1,2}^{X,Y}$ ) were computed as the rms of the positional residuals about the median value, divided by the square root of the number of measurements  $N_{1,2}$ :  $\text{rms}_{1,2}/\sqrt{N_{1,2}}$ . Therefore, the error in each PM-component associated to each star is simply the sum in quadrature between first- and second-epoch errors:  $\sigma_{\text{PM}}^X = \sqrt{(\sigma_1^X)^2 + (\sigma_2^X)^2}/\Delta T$  and  $\sigma_{\text{PM}}^Y = \sqrt{(\sigma_1^Y)^2 + (\sigma_2^Y)^2}/\Delta T$ .

With this first PM determination, we went back

to our original reference-star list and removed those sources whose motion was not consistent with the cluster’s mean motion,  $(0,0)$   $\text{mas yr}^{-1}$  by construction. We repeated the entire procedure three times, after which the number of stars in the reference list stopped changing. To be conservative, we decided to build the final PM catalog taking into account only the 30 546 stars having at least 3 position measurements in each epoch. The typical error for well-exposed stars is smaller than  $0.002$   $\text{pixel yr}^{-1}$  in each coordinate, i.e. smaller than  $0.07$   $\text{mas yr}^{-1}$  as shown in Fig. 2.

We converted the PMs into units of  $\text{mas yr}^{-1}$  by multiplying the measured displacements by the pixel scale of the master frame (previously rescaled to  $0.04''/\text{pixel}$ ) and dividing by the temporal baseline (5.464 yrs). Since the master frame is already oriented according to the equatorial coordinate system, the X PM-component corresponds to that projected along (negative) Right Ascension ( $-\mu_\alpha \cos \delta$ ), while the Y PM-component to that along Declination ( $\mu_\delta$ ). The output of this analysis is summarized in Figure 3, where in the upper panels we show the Vector Point Diagrams (VPDs) and in the lower panels the corresponding CMDs. Close inspections of the VPDs suggest that at least three populations with distinct kinematics can be identified in the direction of NGC 6681.

1. The cluster population is identified by the clump of stars at  $(0,0)$   $\text{mas yr}^{-1}$ . By selecting stars within the blue circle in the second upper panel, a clean CMD of the cluster is obtained (second lower panel of Fig. 3).
2. A secondary clump of stars is located at roughly  $(-4, 3.5)$   $\text{mas yr}^{-1}$ . Stars selected within the red circle in the third upper panel of Fig. 3 define in the CMD (the third lower panel) a sequence significantly fainter than that defined by cluster stars (as already noticed in the previous Section). Therefore, these stars belong to a population that is both kinematically and photometrically different from that of the cluster. This population appears uniformly distributed across the FoV of our observations and thus it can be associated to the Sgr dSph, whose main body is located in the background of NGC 6681.
3. A much sparser population of stars is cen-

tered around  $(-4.5, 0)$   $\text{mas yr}^{-1}$ . The bulk of this population is highlighted with the green circle in the last upper panel of Fig. 3. The corresponding CMD suggests that this is essentially due to fore/background sources.

#### 4. ABSOLUTE PROPER MOTION DETERMINATION

In this section we describe how we determined the absolute reference frame zero point in order to bring our relative PMs (Section 3) into an absolute system.

##### 4.1. Absolute reference frame

In order to measure absolute PMs, an absolute zero point is required. The best option to define this zero point is to use extragalactic sources, since they are essentially stationary on account of their enormous distances. This method has already been adopted in several previous works, such as Dinescu et al. (1999), Bellini et al. (2010), or Sohn et al. (2012). In order to find extragalactic sources we first tried to use the Nasa Extragalactic Database but found that it is incomplete in the innermost regions of dense stellar systems like GCs, and provides no detectable sources in our FoV. We then performed a careful visual inspection of our images. Thirty-one galaxies were identified by eye, but only 11 of them have point-like nuclei and thus are successfully fitted by the adopted PSF. Out of these, we selected only the 5 galaxies with an associated QFIT value (see Anderson & King 2006 for details) smaller than 0.6: this was necessary to guarantee a measurement of the source centroid accurate enough to provide a precise determination of the zero point for the absolute PMs. Figure 4 shows how these galaxies appear in the F814W band.

The selected galaxies are located very close to each other in the relative-PM VPD (Fig. 5), as expected for distant sources. Therefore, we defined the zero-point of the absolute reference frame as the weighted mean of their relative PMs (see the blue dot in Figure 5):

$$(\mu_\alpha \cos \delta, \mu_\delta)_{\text{gals}} = (-1.58 \pm 0.18, 4.57 \pm 0.16) \text{ mas yr}^{-1}, \quad (1)$$

as measured with respect to the mean NGC 6681 motion derived in Section 5.1. The uncertainties

correspond to the error on the calculated weighted means. In order to check whether the quoted uncertainties could be underestimated by taking into account only the individual PM errors, we computed the reduced  $\chi_\nu^2 \equiv \chi^2/(N-1)$  of the scatter of the five galaxies around their weighted mean. The resulting values are  $\chi_\nu^2 = 0.17$  and  $\chi_\nu^2 = 1.29$  for the two PM components respectively. These values suggest a reasonable estimate for the  $\mu_\delta$  component uncertainty, and a possible overestimate of the  $\mu_\alpha \cos \delta$  component error. However, given the small sample of galaxies, the  $\chi^2$  statistics could be not fully reliable. Therefore we maintained the quoted uncertainties throughout the following analysis.

##### 4.2. Systematic error estimates

Since any measurement of absolute PMs relies on the accuracy of the absolute reference frame determination, it is important to look for possible sources of systematic errors and, if any is found, to quantify their impact. One of these sources could be the possible rotation of NGC 6681 on the plane of the sky. Because we used only cluster stars to define the (linear) transformation between each exposure and the reference frame, if the cluster is rotating, then our frame will also be rotating. As such, if NGC 6681 has any component of rotation in the plane of the sky, our procedure would have introduced an artificial rotation (equal in modulus but opposite in sign) to background and foreground objects around the cluster center.

NGC 6681 shows a very small ellipticity ( $\epsilon = 0.01$ ; Harris 1996, 2010 edition). Hence, from the relationship between ellipticity and the rotational parameter  $v_{\text{rot}}/\sigma$  ( $v_{\text{rot}}$  and  $\sigma$  being, respectively, the cluster rotational velocity and velocity dispersion; Illingworth 1977), we can reasonably expect that  $v_{\text{rot}}/\sigma \ll 0.5$  at  $r = r_h$ , with  $r_h$  being the half-light radius, at least for the edge-on component of rotation. If the face-on and edge-on components are similar, we can calculate an upper limit to the rotational velocity of  $v_{\text{rot}} \ll 1.4 \times 10^{-3} \text{ mas yr}^{-1} \text{ arcsec}^{-1}$ , using  $\sigma = 5.2 \text{ km s}^{-1}$ ,  $r_h = 0.71'$  and the distance  $d = 9 \text{ kpc}$  (all from Harris 1996, 2010 edition). This value corresponds to a rotational PM of  $0.084 \text{ mas yr}^{-1}$  at a distance of  $1'$  from the cluster center. This is comparable to the random errors in our absolute astrometry (eq. [1]). Hence we need

to carefully check for the possible presence of a rotational component on the plane of the sky. To this end we selected Sgr dSph members since their small PM dispersion (compared to field stars) produces more stringent limits on the measured rotation values. Note that the Sgr dSph does not rotate (Peñarrubia et al. 2011), at least it should not rotate around the center of NGC 6681. Thus any possible rotation signal would belong to the cluster.

We selected Sgr dSph stars from the CMD (in the intervals  $17.5 < m_{F555W} < 23$  mag and  $1.1 < m_{F555W} - m_{F814W} < 1.8$  mag) and from the VPD, rejecting sources that lay beyond  $1 \text{ mas yr}^{-1}$  from its PM bulk distribution. In addition, we rejected stars with a PM uncertainty larger than  $0.5 \text{ mas yr}^{-1}$ . Seventy three stars survived these selection criteria. We decomposed their PM vectors into radial ( $\mu_{\text{rad}}$ ) and tangential ( $\mu_{\text{tan}}$ ) components with respect to the center of NGC 6681. The resulting distributions of the  $\mu_{\text{rad}}$  and  $\mu_{\text{tan}}$  components as a function of the distance  $r$  from the cluster's center are shown in Figure 6. We fitted these distributions with a straight line, forced through the origin (functional form  $f = mr$ ) since at  $r = 0$  any internal cluster mean motion (rotation in the PM tangential component and contraction/expansion in the radial direction) is zero. We determined the angular coefficient  $m$  by calculating the minimum of the function  $d(\chi^2)/dm$  and we defined the errors using the  $m$ -values corresponding to  $\chi^2 = \chi_{\text{min}}^2 + 1$ . In this approach, we defined  $\chi^2 = \sum (\mu_{\text{obs}} - mr)^2 / \sigma^2$ , where  $\sigma$  is the scatter of the points around the best fit ( $\sim 0.3 \text{ mas yr}^{-1}$ ). Hence, the inferred errors on  $m$  take into account the observed scatter (which includes contributions from the internal velocity dispersion of the Sgr dSph stars), and not merely the formal random errors on the individual PM measurements.

The best fits of the two distributions give the following slope values:  $m_{\mu, \text{rad}} = (0.1 \pm 5.3) \times 10^{-4} \text{ mas yr}^{-1} \text{ arcsec}^{-1}$  and  $m_{\mu, \text{tan}} = (3.2 \pm 4.0) \times 10^{-4} \text{ mas yr}^{-1} \text{ arcsec}^{-1}$ . The fits are shown in Figure 6 with red solid lines (the  $\pm\sigma$  uncertainty in the fit is shown as red dashed lines). Our estimated rotation signal ( $\mu_{\text{tan}} = r \times (3.2 \pm 4.0) \times 10^{-4} \text{ mas yr}^{-1} \text{ arcsec}^{-1}$ ) corresponds to  $v_{\text{rot}} = 0.82 \pm 1.02 \text{ km s}^{-1}$  at  $1'$  from the cluster center, fully consistent with zero. This firmly demonstrates that

the cluster rotation is negligible in the plane of the sky. This contrasts with the case of e.g.  $\omega$  Cen (van de Ven et al. 2006).

Anderson & King (2003) (AK03) estimated the rotation of 47 Tuc from the difference of the motion of the Small Magellanic Cloud (located behind the cluster) in two pointings on opposite sides of the cluster. Similar to AK03, in this work we have used stars in a background association as a zero-rotation reference to obtain very precise limits on the plane-of-sky rotation of a globular cluster. This is the first time, however, that such a measurement has been made using only one observed pointing at the cluster center. We want to stress that this has only been possible thanks to the small dispersion of the Sgr dSph PMs, which translates into a high accuracy in the determination of a possible rotation signal.

Since the rotation turned out to be consistent with zero to within the uncertainties, we can assume that PMs of background galaxies are not affected by any cluster-rotation effect. To be conservative, however, we used the uncertainty on the slope  $m_{\mu, \text{rad}}$  to quantify the possible systematic error on the determination of the absolute reference frame. We computed the radial and tangential components of the PMs of the 5 selected galaxies and added to the tangential motion of each galaxy a term  $b = \pm 4 \times 10^{-4} \times r$  (where  $r$  is the distance of each galaxy from the cluster center). Then we recalculated the weighted-mean relative PM value, which defines the absolute zero point. The difference with respect to the previous determination is  $\Delta|\mu_{\alpha} \cos \delta| = 0.023 \text{ mas yr}^{-1}$  and  $\Delta|\mu_{\delta}| = 0.026 \text{ mas yr}^{-1}$ . These systematic errors on the determination of the absolute reference frame are significantly smaller than the random errors (eq. [1]), and we therefore ignore them in the following.

It is also important to be aware of possible contributions from parallax to measured positional shifts between observations taken at different epochs. Compared to distant background sources, a foreground object will move annually on a parallactic ellipse of semi-major axis length  $p \equiv 0.1$  (10 kpc / d) mas. The positional shift thus introduced between two observations at random times separated by a baseline  $\Delta T$  is at most twice this value. This yields an apparent PM of size  $|\Delta PM| \leq 2p/\Delta T$ . For our NGC 6681 observations,  $r_{\text{md}} = 9 \text{ kpc}$  and  $\Delta T = 5.464 \text{ yr}$ , so that



$|\Delta PM| \leq 0.04 \text{ mas yr}^{-1}$ . This is well below the uncertainties in our absolute reference frame. So while it is not difficult to correct for parallax explicitly, we have not done so in the present context. The Sgr dSph is farther away than NGC 6681, so any systematic errors in its PM due to parallax would be correspondingly smaller.

There are many other possible sources of systematic error that can affect absolute astrometry with *HST*. *HST* is a very stable instrument, and most authors use analysis software that is based on the concepts in Anderson & King (2006). Therefore, most systematic errors should be similar in magnitude between different studies. Sohn et al. (2012, 2013) achieved systematic errors  $\lesssim 0.03 \text{ mas yr}^{-1}$  in studies of M31 and Leo I using techniques that are very similar to those used here. This is significantly smaller than the random errors in our absolute reference frame (see eq. [1]). The fact that our results are not significantly affected by unknown systematics is also supported by comparison of our PM results with those of other authors (see Section 5.2 below), which show good agreement to within the random uncertainties.

## 5. ABSOLUTE PROPER MOTION RESULTS

In this section we present the results for the absolute PMs of the three populations under investigation. Each measurement quoted in the following subsections refers to Figure 7, where the blue crosses correspond to the absolute PM estimate of each population and the blue ellipses to their uncertainty.

### 5.1. NGC 6681

In order to measure the absolute PM of NGC 6681 we selected only stars  $1.0 \text{ mas yr}^{-1}$  from the cluster mean motion and in the magnitude interval  $17.5 < m_{F555W} < 22.5 \text{ mag}$ . We iteratively refined the selection by applying a  $3\sigma$  rejection and re-calculating the barycenter of the PMs as the weighted mean value of the PMs of the selected stars, until the difference between two subsequent steps was smaller than  $0.01 \text{ mas yr}^{-1}$ . After the last iterative step, a total of  $N_{clu} = 14030$  stars survived the selection criteria. We used the sum in quadrature between each single measurement

error and the velocity dispersion of the cluster  $\sigma_v = 0.12 \text{ mas/yr}$  (based on the line-of-sight velocity dispersion and distance given by Harris 1996) as weights. To estimate the error  $\Delta PM$  on the weighted mean PM in each coordinate we use the standard error-in-the-mean, i.e., the dispersion of the surviving stars around the weighted mean PM, divided by  $\sqrt{(N_{clu}-1)}$ . This includes scatter from the internal dispersion of NGC 6681 stars, which therefore does not need to be estimated explicitly. We find that the resulting error  $\Delta PM$  is negligible compared to the error on the absolute reference frame. Therefore, the latter dominates the uncertainty on the final absolute PM of NGC 6681, which is:

$$(\mu_\alpha \cos \delta, \mu_\delta) = (1.58 \pm 0.18, -4.57 \pm 0.16) \text{ mas yr}^{-1}. \quad (2)$$

The PM derived here can be combined with the known distance and line-of-sight velocity of NGC 6681 from Harris (1996), to determine the motion of the cluster in the Galactocentric rest frame. Using the same formalism, conventions, and solar motion as in van der Marel et al. (2012), this yields  $(V_X, V_Y, V_Z) = (203 \pm 2, 111 \pm 9, -179 \pm 7) \text{ km s}^{-1}$ . This corresponds to a total Galactocentric velocity  $|\vec{V}| = 292 \pm 5 \text{ km s}^{-1}$ . This significantly exceeds the central velocity dispersion  $\sigma \approx 120 \text{ km s}^{-1}$  of the Milky Way's spheroidal components (e.g., Deason et al. 2012). Hence, NGC 6681 must spend most of the time along its orbit at significantly larger distances from the Galactic Center than its current distance of 2.2 kpc (Harris 1996).

### 5.2. Sagittarius Dwarf Galaxy

In order to determine the absolute PM of the Sgr dSph we basically followed the same procedure previously described for NGC 6681. In setting the weights for the PM averaging, we used the dispersion  $\sigma_v \sim 0.3 \text{ mas yr}^{-1}$  implied by Figure 6. This includes both contributions from the internal velocity dispersion of the Sgr dSph (see e.g. Frinchaboy et al. 2012), and unquantified systematic errors. We selected stars within  $1.0 \text{ mas yr}^{-1}$  from the Sgr dSph mean motion and in the interval  $17.5 < m_{F555W} < 23.5$ , which is one magnitude fainter with respect to the case of NGC 6681, since most of the Sgr dSph stars belong to its faint MS. The resulting absolute PM

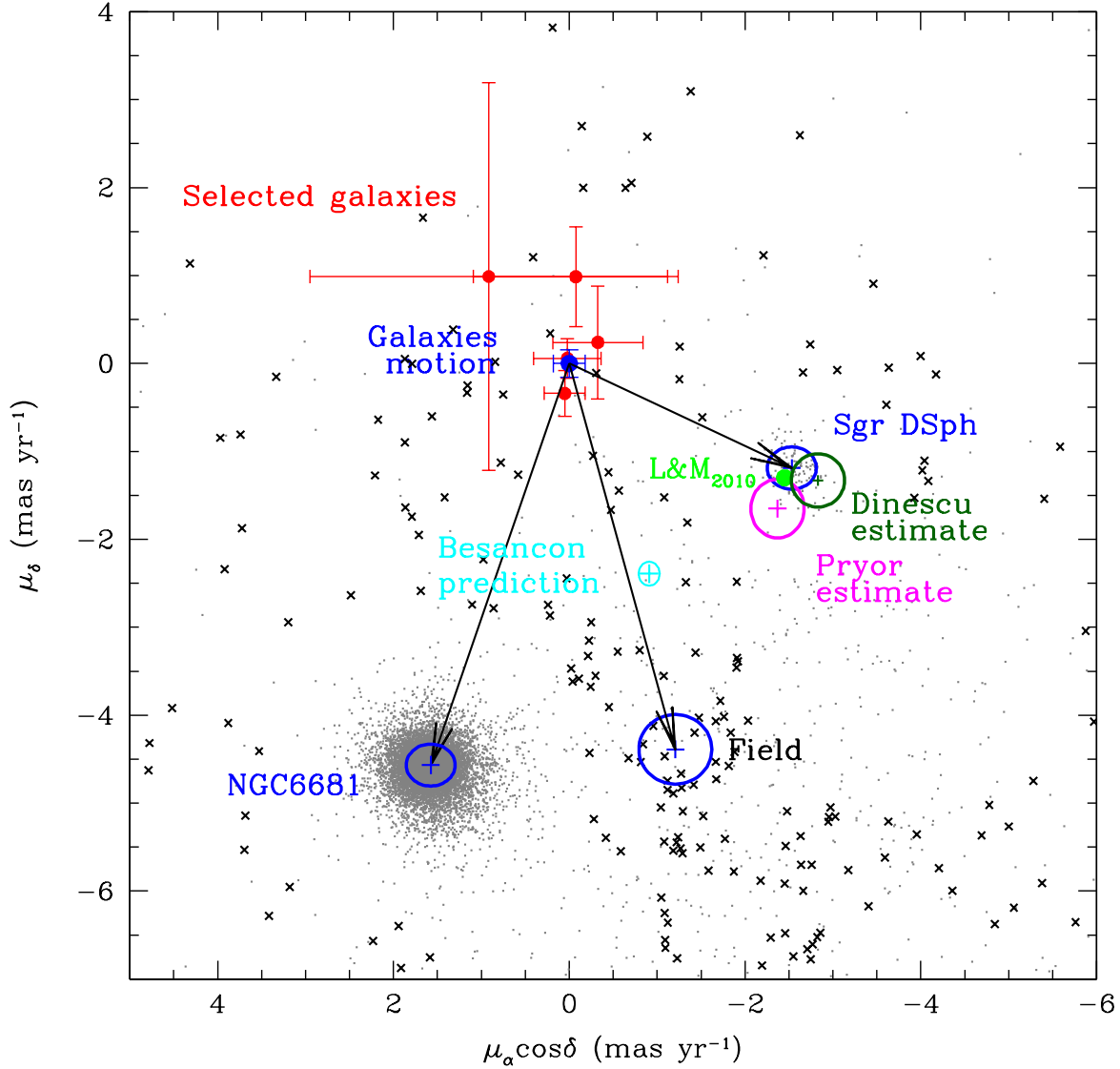


Fig. 7.— VPD of the absolute PMs. The red dots indicate the selected background galaxies (see also Fig. 5), whose mean motion corresponds to the zero point of the VPD. The blue ellipses are centered on the measured absolute PMs of the three populations (marked with a blue cross) and their size corresponds to the calculated 68.3% confidence region. The black arrows indicate their absolute PM vectors. In the proximity of the Sgr dSph estimate, the PM value predicted by Law & Majewski (2010) is shown as a light green dot, while the Pryor et al. (2010) and Dinescu et al. (2005) measurements and their 68.3% confidence regions are shown as magenta and dark green ellipses, respectively. Finally, the cyan ellipse describes the prediction on the PM of the field population by the Besançon model, which differs from our estimate obtained using the stars in the same magnitude and color range (marked with black crosses, see the text for the selection criteria).

is:

$$(\mu_\alpha \cos \delta, \mu_\delta) = (-2.54 \pm 0.18, -1.19 \pm 0.16) \text{ mas yr}^{-1}. \quad (3)$$

We compared this value with previous es-

timates. With the aim of reconstructing the kinematical history of this galaxy and to predict its evolution in a triaxial Milky Way halo, Law & Majewski (2010) built a N-body model able to reproduce most of the system’s observed properties. In the Law & Majewski model, the Sgr dSph has a Galactocentric motion  $(V_X, V_Y, V_Z) = (230, -35, 195) \text{ km s}^{-1}$ , corresponding to a total velocity  $|\vec{V}| = 304 \text{ km s}^{-1}$ . The absolute PM predicted by the model is  $(\mu_\alpha \cos \delta, \mu_\delta) = (-2.45, -1.30) \text{ mas yr}^{-1}$  (light green dot in Figure 7). An estimate of the absolute PM of the Sgr dSph based on *HST* data has been recently presented by Pryor et al. (2010). The authors used foreground Galactic stellar populations as reference frame and they determined an absolute PM of  $(\mu_\alpha \cos \delta, \mu_\delta) = (-2.37 \pm 0.2, -1.65 \pm 0.22) \text{ mas yr}^{-1}$ , which is shown as a magenta ellipse in Figure 7. A ground-based estimate of the absolute PM of the Sgr dSph was presented by Dinescu et al. (2005). Using the Southern Proper Motion Catalog 3 they determined that  $(\mu_\alpha \cos \delta, \mu_\delta) = -2.83 \pm 0.20, -1.33 \pm 0.20) \text{ mas yr}^{-1}$ , which is shown as the dark green ellipse in Figure 7. These previous estimates are in rough agreement with the value determined here.

It is worth noting, however, that these other determinations are not directly comparable with ours, since they refer to different regions of the Sgr dSph. Indeed, this has two possible effects. The first one is that possible internal motions, such as rotation, could translate into different mean motions, thus introducing a systematic effect. This should not be a problem for the Sgr dSph, since this galaxy does not show any evidence of rotation (Peñarrubia et al. 2011). The second effect is that if the whole galaxy has a 3D velocity vector different from zero, then the observed PMs for different pointings are not the same, because of perspective effects due to the imperfect parallelism between the lines of sight (van der Marel et al. 2002). Since the Sgr dSph is a nearby galaxy, this effect could be relevant and we calculated the correction to apply (as in van der Marel & Guhathakurta 2008) in order to obtain comparable estimates at the center of mass of the Sgr dSph.

Under the hypothesis that the center of mass of the Sgr dSph is moving as the Law & Majewski (2010) prediction, our perspective-corrected PM

measurement becomes  $(\mu_\alpha \cos \delta, \mu_\delta) = (-2.56 \pm 0.18, -1.29 \pm 0.16) \text{ mas yr}^{-1}$ . The corrected Pryor et al. (2010) estimate becomes  $(\mu_\alpha \cos \delta, \mu_\delta) = (-2.37 \pm 0.20, -1.63 \pm 0.22) \text{ mas yr}^{-1}$ , and the corrected Dinescu et al. (2005) estimate becomes  $(\mu_\alpha \cos \delta, \mu_\delta) = -2.83 \pm 0.20, -1.56 \pm 0.20) \text{ mas yr}^{-1}$ . Thus our measurement is consistent with the previous observations. The weighted average of all observational estimates of the center-of-mass PM of the Sgr dSph is  $(\mu_\alpha \cos \delta, \mu_\delta) = (-2.59 \pm 0.11, -1.45 \pm 0.11) \text{ mas yr}^{-1}$ . This is consistent with the theoretical model of Law & Majewski (2010), once the uncertainties on transforming that into a PM value (e.g., from uncertainties in the distance and solar motion) are taken into account as well. Therefore, our measurement is consistent within about a  $1\sigma$  uncertainty both with theoretical predictions (Law & Majewski 2010) and the previous *HST* observations (Pryor et al. 2010).

### 5.3. Field

We compared the absolute PMs of Field stars in our catalog with those predicted in the same region of sky by the Besançon Galactic model (Robin et al. 2003). We generated a simulation over a 0.01 square degrees ( $6' \times 6'$ ) FoV around the center of NGC 6681 ( $l = 2^\circ.85, b = -12^\circ.51$ ) and 50 kpc deep. To minimize any possible bias, we have constructed a sample as similar as possible to the observed stars, based on a comparison between the observed and the simulated CMDs. Simulated field stars were selected within the magnitude range:  $17.5 < m_{F555W} < 22.5 \text{ mag}$  and  $(m_{F555W} - m_{F814W}) > 1.5 \text{ mag}$  and 1378 stars survived these criteria. The average predicted motion is shown in Figure 7 as a cyan ellipse, which corresponds to  $(\mu_\alpha \cos \delta, \mu_\delta) = (-0.91 \pm 0.08, -2.39 \pm 0.09) \text{ mas yr}^{-1}$ .<sup>3</sup>

Field stars in our observed catalog were selected following the same color and magnitude cuts. We also required these stars to have PM errors smaller than  $0.2 \text{ mas yr}^{-1}$  in each coordinate. Finally, we excluded those stars within  $1.8 \text{ mas yr}^{-1}$  of the cluster mean motion and within  $1.0 \text{ mas yr}^{-1}$  of the

<sup>3</sup>It would be easy to reduce the random uncertainty on this model prediction by drawing a larger number of simulated stars. However, we have not pursued this since the accuracy of the prediction is dominated largely by systematic errors in the model assumptions anyway.

Sgr dSph mean motion. We iteratively removed field stars in symmetric locations with respect to the Sgr dSph and NGC 6681 exclusions in order to better define the mean motion of the Field population and adjusted the weighted mean motion after each iteration (thus following the method described by Anderson & van der Marel 2010 for the determination of the center of  $\omega$  Cen). The 281 selected field stars used for the final estimate are shown as black crosses in Figure 7. Since these stars display a large scatter in the VPD due to their velocity dispersion and not to their random errors, in this case we computed a statistically more appropriate  $3\sigma$ -clipped unweighted mean motion. It is shown as a blue ellipse in Figure 7 and its value is:

$$(\mu_\alpha \cos \delta, \mu_\delta) = (-1.21 \pm 0.27, -4.39 \pm 0.26) \text{ mas yr}^{-1}. \quad (4)$$

Our PM measurement is similar to the prediction of the Besançon model, in that it points in the same direction on the sky (see Figure 7). However, the sizes of the PM vectors are not formally consistent to within the random errors. Since our measurements for Sgr dSph stars are entirely consistent with both previous measurements and theoretical predictions, this cannot be due to systematic errors in our measurements (which would affect all point sources equally). Instead, the mismatch is most likely due to shortcomings in the Besançon models. In particular, for pointings this close to the Galactic Plane, the model predicted PM distribution is likely to depend sensitively on the adopted dust extinction model, which is poorly constrained observationally. Also, the model predicted PM distribution depends on the solar motion in the Milky Way, which continues to be debated (e.g., McMillan 2011; Bovy et al. 2012).

## 6. CONCLUSIONS

We have analyzed two sets of *HST* observations separated by a temporal baseline of 5.464 years in the direction of the Galactic GC NGC 6681 in order to obtain the first-ever measurement of its absolute PM, as well as the absolute motions of the Sgr dSph and the field population in this direction. First, we obtained relative PMs for a total of about 30 000 sources. For the brighter ones, the uncertainties are smaller than  $\sim 0.07$  mas yr $^{-1}$  in each coordinate. Then, by using back-

ground galaxies, we determined the zero-point of the absolute-motion reference frame with an uncertainty of 0.18 and 0.16 mas yr $^{-1}$  on the  $\mu_\alpha \cos \delta$  and  $\mu_\delta$  components, respectively. We also quantified the systematic errors on the definition of the absolute reference frame due to possible internal rotation of NGC 6681. We demonstrated that very stringent constraints on the rotation of a GC can be obtained by using non-member populations, provided that their PMs have a sufficiently small dispersion. We used Sgr dSph stars as the non-member population and we estimated a rotational velocity for NGC 6681 of  $v_{\text{rot}} = 0.82 \pm 1.02$  km s $^{-1}$  at 1' from the cluster center, consistent with zero. This corresponds to negligible systematic errors of (0.023, 0.026) mas yr $^{-1}$  in the previously quoted PM components.

We measured the absolute PM for the three populations under investigation. The absolute PM of NGC 6681 is  $(\mu_\alpha \cos \delta, \mu_\delta) = (1.58 \pm 0.18, -4.57 \pm 0.16)$  mas yr $^{-1}$ . We also measured the absolute PM of the Sgr dSph and compared it with previous determinations and model predictions. Our estimate is  $(\mu_\alpha \cos \delta, \mu_\delta) = (-2.57 \pm 0.18, -1.14 \pm 0.16)$  mas yr $^{-1}$ . After correction for viewing perspective to obtain an estimate of the PM of the Sgr dSph center of mass, this value is consistent within about a  $1\sigma$  uncertainty with both the model prediction of Law & Majewski (2010) and the perspective corrected measurements of Pryor et al. (2010) and Dinescu et al. (2005). Finally, we estimated the absolute PM of the field population intercepted along the line of sight to be  $(\mu_\alpha \cos \delta, \mu_\delta) = (-1.17 \pm 0.27, -3.99 \pm 0.26)$  mas yr $^{-1}$ .

This research is part of the project COSMIC-LAB (web site: [www.cosmic-lab.eu](http://www.cosmic-lab.eu)) funded by the European Research Council (under contract ERC-2010-AdG-267675). Support for this work was provided by NASA through a grant for program AR-12845 from the Space Telescope Science Institute (STScI), which is operated by the Association of Universities for Research in Astronomy (AURA), Inc., under NASA contract NAS5-26555.

## REFERENCES

Anderson, J., & King, I. R. 2003, *AJ*, 126, 772

- Anderson, J., & King, I., STScI Inst. Sci. Rep. ACS 2006-01 (Baltimore: STScI)
- Anderson, J., Bedin, L. R., Piotto, G., Yadav, R. S., & Bellini, A. 2006, *A&A*, 454, 1029
- Anderson, J. 2007, Instrument Science Report ACS 2007-08, 12 pages, 8
- Anderson, J., Sarajedini, A., Bedin, L. R., et al. 2008, *AJ*, 135, 2055
- Anderson, J., & Bedin, L. R. 2010, *PASP*, 122, 1035
- Anderson, J., & van der Marel, R. P. 2010, *ApJ*, 710, 1032
- Anderson, J., MacKenty, J., Baggett S., et al. 2012, WFC3/ISR 2012-2013 (Baltimore, MD: STScI)
- Bellazzini, M., Ferraro, F. R., & Ibata, R. 2003, *AJ*, 125, 188
- Bellazzini, M., Ferraro, F. R., & Buonanno, R. 1999, *MNRAS*, 307, 619
- Bellini, A., Bedin, L. R., Pichardo, B., et al. 2010, *A&A*, 513, A51
- Bellini, A., Anderson, J., & Bedin, L. R. 2011, *PASP*, 123, 622
- Bovy, J., Allende Prieto, C., Beers, T. C., et al. 2012, *ApJ*, 759, 131
- Casetti-Dinescu, D. I., Girard, T. M., Herrera, D., et al. 2007, *AJ*, 134, 195
- Casetti-Dinescu, D. I., Girard, T. M., Korchagin, V. I., van Altena, W. F., & López, C. E. 2010, *AJ*, 140, 1282
- Clarkson, W., Sahu, K., Anderson, J., et al. 2008, *ApJ*, 684, 1110
- Deason, A. J., Belokurov, V., Evans, N. W., & An, J. 2012, *MNRAS*, 424, L44
- Dinescu, D. I., Girard, T. M., van Altena, W. F., Mendez, R. A., & Lopez, C. E. 1997, *AJ*, 114, 1014
- Dinescu, D. I., Girard, T. M., & van Altena, W. F. 1999, *AJ*, 117, 1792
- Dinescu, D. I., Girard, T. M., van Altena, W. F., & López, C. E. 2005, *ApJ*, 618, L25
- Debattista, V. P., Roskar, R., Valluri, M., et al. 2013, arXiv:1301.2670
- Deg, N., & Widrow, L. 2013, *MNRAS*, 428, 912
- Ferraro, F. R., Dalessandro, E., Mucciarelli, A., et al. 2009, *Nature*, 462, 483
- Ferraro, F. R., Beccari, G., Dalessandro, E., et al. 2009, *Nature*, 462, 1028
- Ferraro, F. R., Lanzoni, B., Dalessandro, E., et al. 2012, *Nature*, 492, 393
- Forbes, D. A., & Bridges, T. 2010, *MNRAS*, 404, 1203
- Frinchaboy, P. M., Majewski, S. R., Muñoz, R. R., et al. 2012, *ApJ*, 756, 74
- Goldsbury, R., Richer, H. B., Anderson, J., et al. 2010, *AJ*, 140, 1830
- Harris, W. E. 1996, *AJ*, 112, 1487
- Ibata, R. A., Gilmore, G., & Irwin, M. J. 1994, *Nature*, 370, 194
- Illingworth, G. 1977, *ApJ*, 218, L43
- Law, D. R., Johnston, K. V., & Majewski, S. R. 2005, *ApJ*, 619, 807
- Law, D. R., & Majewski, S. R. 2010, *ApJ*, 714, 229
- McMillan, P. J. 2011, *MNRAS*, 414, 2446
- Norris, J. E., & Da Costa, G. S. 1995, *ApJ*, 447, 680
- Peñarrubia, J., Zucker, D. B., Irwin, M. J., et al. 2011, *ApJ*, 727, L2
- Platais, I., Girard, T. M., Kozhurina-Platais, V., et al. 1998, *AJ*, 116, 2556
- Pryor, C., Piatek, S., & Olszewski, E. W. 2010, *AJ*, 139, 839
- Robin, A. C., Reylé, C., Derrière, S., & Picaud, S. 2003, *A&A*, 409, 523
- Sarajedini, A., Bedin, L. R., Chaboyer, B., et al. 2007, *AJ*, 133, 1658

- Siegel, M. H., Majewski, S. R., Law, D. R., et al.  
2011, ApJ, 743, 20
- Sohn, S. T., Anderson, J., & van der Marel, R. P.  
2012, ApJ, 753, 7
- Sohn, S. T., Besla, G., van der Marel, R. P., et al.  
2013, ApJ, 768, 139
- Ubeda, L., Anderson, J., STScI Inst. Sci. Rep.  
ACS 2012-03 (Baltimore: STScI)
- van de Ven, G., van den Bosch, R. C. E., Verolme,  
E. K., & de Zeeuw, P. T. 2006, A&A, 445, 513
- van der Marel, R. P., Alves, D. R., Hardy, E., &  
Suntzeff, N. B. 2002, AJ, 124, 2639
- van der Marel, R. P., & Guhathakurta, P. 2008,  
ApJ, 678, 187
- van der Marel, R. P., Fardal, M., Besla, G., et al.  
2012, ApJ, 753, 8
- Zinn, R., ASP Conf. Ser. 48, The Globular  
Cluster-Galaxy connection, ed. G.H. Smith &  
J.P. Brodie (San Francisco, CA:ASP), 38